

Role of milk fat globule-epidermal growth factor 8 in colonic inflammation and carcinogenesis

Ryusaku Kusunoki¹, Shunji Ishihara¹, Yasumasa Tada¹, Akihiko Oka¹, Hiroki Sonoyama¹, Nobuhiko Fukuba¹, Naoki Oshima¹, Ichiro Moriyama^{1,2}, Takafumi Yuki^{1,3}, Kousaku Kawashima¹, Md. Mesbah Uddin Ansary¹, Yoshitsugu Tajima⁴, Riruke Maruyama⁵, Toru Nabika⁶, Yoshikazu Kinoshita¹

¹Department of Internal Medicine II, Shimane University Faculty of Medicine, Japan

²Cancer Center, Shimane University Hospital, Japan

³Division of Gastrointestinal Endoscopy, Shimane University Hospital, Japan

⁴Department of Digestive and General Surgery, Shimane University Faculty of Medicine

⁵Department of Organ Pathology, Shimane University Faculty of Medicine, Shimane, Japan

⁶Department of Functional Pathology, Shimane University Faculty of Medicine, Japan

Short running title: MFG-E8 and intestinal carcinogenesis

Key words: MFG-E8, inflammatory bowel disease, intestinal inflammation, colitic cancer, colon cancer

Address for correspondence:

Shunji Ishihara, M.D., Ph.D.

Department of Internal Medicine II

Shimane University Faculty of Medicine

89-1, Enya-cho, Izumo, Shimane, Japan

Tel: +81-853-20-2190

Fax: +81-853-20-2187

E-mail: si360405@med.shimane-u.ac.jp

Abstract

Background: MFG-E8 promotes phagocytic clearance of apoptotic cells to maintain normal tissue homeostasis. However, its functions in intestinal inflammation and carcinogenesis are unknown. **Methods:** Experimental colitis was induced in MFG-E8 knockout (KO) and wild-type (WT) mice by DSS administration. Colon tissues were used for assessments of colitis activity and epithelial proliferation. A mouse colitis associated cancer (CAC) model was induced by intraperitoneal injection of azoxymethane (AOM), then the animals were given a single administration of DSS. A sporadic colon cancer model was established by repeated intraperitoneal injections of AOM. The role of MFG-E8 in epithelial proliferation with or without treatment of siRNA targeting α_v -integrin was examined *in vitro* using a WST-1 assay. **Results:** The severity of colitis in KO mice was greater than that in WT mice, while the proliferative potential of colonic epithelial cells in KO mice was lower during the regenerative phase. In both CAC and sporadic models, tumor size in KO was lower as compared to WT mice, while decreased tumor incidence was only found in the CAC model. *In vitro* findings showed that MFG-E8 promotes epithelial cell proliferation, and treatment with a siRNA targeting α_v -integrin reduced the proliferation of Colon-26 cells stimulated with recombinant MFG-E8. **Conclusions:** MFG-E8 promotes tumor growth regardless of the presence or absence of colonic inflammation, whereas colon tumor development is initiated by MFG-E8 under inflammatory condition. These MFG-E8 functions may be dependent on integrin-mediated cellular signaling.

Introduction

Engulfment of apoptotic cells, an essential process to avoid release of dangerous and inflammatory mediators, is regulated by a variety of molecular mechanisms for maintaining immune homeostasis (1-5). Milk fat globule-epidermal growth factor 8 (MFG-E8), a secreted glycoprotein, forms a link between phosphatidylserine (PS) on apoptotic cells and $\alpha_v\beta_3$ -integrin on phagocytes for enhancing clearance of those cells (2, 3). This glycoprotein is an essential molecule for preventing abnormal immune activation under physiological conditions (6, 7). Deficiency or dysfunction of MFG-E8 leads to accumulation of apoptotic cells in various organs, which is involved in the development of several immune-mediated disorders (8-12).

Apart from its function for apoptotic cell clearance, MFG-E8 also directly regulates a variety of cellular functions under various disease conditions. In particular, its anti-inflammatory effects in the intestinal tract have been recently reported (13-17). Our previous study revealed that MFG-E8 down-regulates an inflammatory function of macrophages via $\alpha_v\beta_3$ -integrin-dependent phosphorylated focal adhesion kinase (pFAK) signaling, which contributed to reduction of intestinal inflammation in dextran sodium sulfate (DSS)- and trinitrobenzene sulfonic acid (TNBS)-induced colitis models (15-17). In addition, other studies have demonstrated that MFG-E8 attenuates intestinal inflammation triggered by sepsis and ischemic-reperfusion (I/R) in several animal models (18-22).

In addition to an anti-inflammatory role, MFG-E8 enhances cell proliferation and migration, as well as anti-apoptosis and vascularization processes, which contribute to regeneration and repair of damaged tissues in various organs (20, 23, 24). On the other hand, those functions are also closely associated with malignant cell growth and

tumor progression. Previous studies have shown MFG-E8 overexpression in several malignancies including breast and bladder cancers, and melanoma, which stimulates tumor cell growth in an autocrine or paracrine manner (25-27). MFG-E8 also promotes tumor cell invasion and metastasis by enhancing expression of angiogenesis factors, as well as down-regulating host tumor immunity (28-30). However, its role in the pathogenesis of colon cancer remains largely unknown. In particular, there are no reports regarding the role of MFG-E8 in development of colitis-associated colon cancer.

In the present study, we employed MFG-E8 knockout (KO) mice to examine the effect of MFG-E8 on colonic inflammation as well as its relationship to colon cancer development, and compared those findings to results obtained with wild type (WT) mice. We found that a deficiency of MFG-E8 significantly reduced tumor incidence and growth in a colitis-associated cancer (CAC) model, while MFG-E8-dependent tumor growth was also confirmed in a sporadic colon cancer model. Furthermore, the proliferating potential of MFG-E8 was shown to be dependent on the cell surface expression of $\alpha_v\beta_3$ -integrin on epithelial cells. These findings raise the possibility that blockade of MFG-E8 or its receptor may become a novel therapeutic option for colon cancer.

Materials and methods

Reagents

Dextran sodium sulfate (DSS, 5 kDa; Wako Pure Chemicals, Osaka, Japan), azoxymethane (AOM; Sigma, St Louis, MO, USA), recombinant mouse MFG-E8 (R&D Systems, Minneapolis, Alabama, USA), and Lipofectamine 2000 (Invitrogen, Carlsbad, CA, USA) were acquired from their respective suppliers. The antibodies used were anti-mouse Proliferation Cell Nuclear Antigen (PCNA) (Dako, Tokyo, Japan), anti-human MFG-E8 antibody (Santa Cruz Biotechnology, Inc, CA), anti-mouse integrin alpha 5 (Abcam, Cambridge, UK) and anti-mouse Ki67 (Abcam).

Mice

Mfge8^{-/-} mice with a C57BL/6 genetic background were obtained from RIKEN BRC, while WT C57BL/6N mice (males, 6-8 weeks old) were purchased from Charles River Japan, Inc. (Kanagawa, Japan). The animals were cared for and handled in accordance with guidelines from the National Institutes of Health and Institute for Animal Experimentation of Shimane University, including housing under constant environmental conditions with circadian light-dark cycles.

Colitis induction and analysis

To produce an acute DSS colitis model, a group of mice was fed 2.5% DSS in drinking water for 10 days, while the control group received only normal drinking water throughout the experimental period. Body weight (BW) was recorded as a parameter for colitis evaluation. After the colitis induction period, the mice were euthanized at various experimental time points and the colons were measured with a ruler on a nonabsorbent

surface. Furthermore, colonic tissues were dissected for histological, real-time PCR, and enzyme immune assays.

Histological examinations

Tissues were formalin fixed and embedded in paraffin blocks. For histological examinations, 3- μ m paraffin sections were stained with hematoxylin and eosin to visualize their general morphology under a light microscope. Histological grading was evaluated as previously described (31). In each histological examination, 3 different parameters were considered: severity of inflammation (based on polymorphonuclear neutrophil infiltration; 0–3: none, slight, moderate, severe), depth of injury (0–3: none, mucosal, mucosal and submucosal, transmural), and crypt damage (0–4: none, basal one-third damaged, basal two-thirds damaged, only surface epithelium intact, entire crypt and epithelium lost). The score for each parameter was multiplied by a factor reflecting the percentage of tissue involvement. ($\times 1$, 0–25%; $\times 2$, 26–50%; $\times 3$, 51–75%; $\times 4$, 76–100%), then all values were added to a sum, with a maximum possible score of 40.

RNA extraction and real time-PCR

Total RNA was extracted from each sample using an RNeasy Protect Mini Kit (Qiagen Inc., Tokyo, Japan), then equal amounts of RNA were reverse transcribed into cDNA using a QPCR cDNA Kit (Stratagene, La Jolla, CA, USA). All primers utilized were flanked by intron-exon junctions using the NCBI blast tool and Primer3 software (Supple Table 1). Quantitative real-time PCR was performed using an ABI PRISM 7700 sequence detection system with SYBR Green PCR master mix (Applied Biosystems,

Foster City, CA, USA), according to the manufacturer's instructions. The levels of mRNA were normalized to that of GAPDH using sequence detector software (Applied Biosystems).

Tumor induction and analysis

We utilized 2 models of murine colon cancer. The first model was established by AOM injection combined with DSS administration, in other words a CAC models. Mice were treated with 10 mg/kg of AOM followed by a single cycle of 2.0% DSS over 7 days, then euthanized at 18 weeks after starting the experiment (32-34). The second model was established by repeated AOM injections without DSS, in other words a sporadic cancer model. Mice were treated with 10 mg/kg of AOM weekly for 6 weeks, then euthanized at 31 weeks after starting the administrations (34-36). Extirpated colons were fixed in 10% neutral buffered formalin for 24 hours, then stained with 0.2% methylene blue (Sigma) for 15 minutes. Tumors were examined using a stereomicroscope at $\times 10$ and $\times 40$ magnifications, and sizes were calculated using Scion Image for Windows (Scion Corporation). After the microscopic examination, colon tissues were embedded in paraffin blocks, and stained with hematoxylin and eosin for histology.

Immunohistochemistry

Mouse colonic tissue samples were used for detection of PCNA and Ki67. To evaluate MFG-E8 expression in human colonic mucosa, multiple endoscopic biopsy specimens were obtained from both active and inactive mucosa of UC patients. In addition, human colon cancer and adenoma tissue samples were obtained by surgery or endoscopic

resection. Immunohistochemistry was performed using formalin-fixed paraffin-embedded blocks. After deparaffinization, endogenous peroxidase activity was blocked with Peroxidase-Blocking Solution (Dako) for 10 minutes. Sections (5 μm thick) were washed with PBS and incubated with an anti-human MFG-E8 antibody (Santa Cruz Biotechnology) at room temperature for 30 minutes. After washing again with PBS, the bound antigen-antibody complex was detected using a ChemMate™ DAKO EnVision™ Detection Kit (DAKO). The study protocols were approved by the ethics committee of Shimane University Faculty of Medicine.

Cell culture

The mouse colon cancer cell line Colon-26 was obtained from American Type Culture Collection (ATCC, Manassas, VA). We previously reported that Colon-26 cells express $\alpha_v\beta_3$ -integrin and respond well to treatment with rMFG-E8 *in vitro* (15), thus they were used for the present *in vitro* assays. Cells were seeded at 2×10^5 cells per ml, and grown in RPMI 1640 medium (Invitrogen) and penicillin-streptomycin-amphotericin B (Invitrogen), then maintained at 37°C in 5% CO₂ in a humidified incubator.

Cell counting assay

Cells were seeded into 24-well plates and harvested 24 hours later using trypsinization, then 100- μl cell suspensions were subjected to counting with Neubauer hemacytometer (Erma, Tokyo, Japan).

WST-1 assay

A 2-(4-iodophenyl)-3-(4-nitrophenyl)-5-(2,4-disulfophenyl)-2H-tetrazolium,

monosodium salt (WST-1) cell proliferation assay is based on enzymatic cleavage of the tetrazolium salt WST-1 to formazan by cellular mitochondrial dehydrogenases present in viable cells. WST-1 assays of Colon-26 cells were performed as described in the product manual (Roche, Mannheim, Germany). Formazan dye produced by viable cells was quantified by measuring absorbance at a wavelength of 450 nm.

RNA interference and transfection

Colon-26 cells were cultured in 6-well plates (2×10^5 cell /ml), then custom siRNAs (Qiagen, Valencia, CA, USA) targeting the mouse α_v integrin gene were transfected (10 nM/well), according to the manufacturer's protocol. After transfection, cells were harvested using trypsinization. The efficiency of target gene knockdown was assessed by real-time PCR and the results were compared to those obtained with the negative control siRNA-transfected condition.

Statistical analysis

All results are expressed as the mean with the standard error of the mean (SEM) or as a range when appropriate. Student's t-test was used as appropriate to examine significant differences. *P* values less than 0.05 were considered to be significant. All statistical analyses were performed using Statistical Analysis Software (SPSS, version 12.0 for the PC; SPSS Japan, Inc.).

Results

BW change and colon morphology of MFG-E KO mice under physiological conditions

A previous study showed that MFG-E8 KO mice spontaneously develop lupus-like autoimmune nephritis due to impaired phagocytosis of apoptosis cells (Hanayama, *et al*, 2004). However, little is known regarding the morphology of the intestinal tract in KO mice under physiological conditions. In this regard, we first examined age-related changes in BW (5~30 weeks), and colon length and histology (6 and 30 weeks) in both KO and WT mice without inflammatory induction, and did not detect any differences for these parameters between those groups (Fig. 1A-E). In addition, the potential of epithelial proliferation was investigated in histological sections by PCNA staining. The number of PCNA-positive epithelial cells in KO mice was higher than that in WT mice (Fig. 1F and 1G).

MFG-E8 protects against DSS-induced colonic inflammation

We recently reported that DSS-induced colonic inflammation was severe in MFG-E8 KO mice (16). In the present study, we modified the experimental design and re-examined the influence of MFG-E8 deficiency on DSS-induced colitis, with those results shown in Figure 2. The deficiency of MFG-E8 exacerbated several colitis parameters including BW loss, histological score, and colonic expression of inflammatory cytokines, which confirmed results recently reported by our group.

Low incidence and growth of CAC in MFG-E8 KO mice

It has been reported that chronic colitis leads to development of CAC (37-39). Notably,

CAC more easily develops as colonic inflammation becomes severe. Since MFG-E8 KO mice show severe colitis (Fig. 2), we speculated that they might be more susceptible to development of CAC than WT mice. A mouse CAC model was induced by intraperitoneal injection of AOM, then the mice were given a single cycle administration of DSS (Fig. 3A). Representative images of colon tumors and their histological appearance are shown in Figure 2B. Contrary to our speculation, the average number of colon tumors in the KO mice was significantly lower than that in the WT mice, while the average tumor size per mouse was also lower in KO mice (Fig. 3C). These findings suggest that a lack of MFG-E8 reduces inflammation-associated tumor development as well as tumor growth even in the presence of severe colitis.

Increased expression of MFG-E8 and its association with epithelial cell proliferation

To confirm the role of MFG-E8 in CAC development, we established DSS-induced colitis in WT and KO mice (Fig. 4A), and investigated the time course changes of MFG-E8 expression in colonic tissues in the mouse models. Colonic expression of MFG-E8 was significantly increased in the WT mice during the regeneration phase of DSS-induced colitis (Fig. 4B). Next, we performed PCNA and Ki67 staining of colonic histological sections to assess proliferation of epithelial cells in WT and KO mice, with representative images of stained colonic PCNA and Ki67 tissues shown in Figure 4C and Supplementary Figure 1A (3 weeks). The prevalence of PCNA- and Ki67-positive epithelial cells was significantly greater in the WT mice as compared to the KO mice (Fig. 4D and Supple. Fig. 1B).

Decreased growth of colon tumors in sporadic colon cancer model of MFG-E8 KO

Mice

Next, we examined whether a lack of MFG-E8 has an influence on tumor incidence and growth in a sporadic colon cancer model. This model was established by repeated AOM injections without DSS administration (Fig. 5A), then the mice were euthanized at 31 weeks. Representative images of colon tumors and their histological appearance are shown in Figure 5B and C. Although we did not find significant differences regarding the number of tumors between the KO and WT mice, the average tumor size per mouse was significantly lower in the former (Fig. 5D).

Increased expression of MFG-E8 in inflammatory colonic mucosa of UC patients

We performed immunohistochemical analysis using colonic tissue sections of UC patients to confirm MFG-E8 localization, which revealed its presence in lamina propria mononuclear cells (Fig. 6A). MFG-E8 expression was significantly higher in active mucosa as compared to inactive mucosa (Fig. 6B).

MFG-E8 expression in human colon cancer cells

Previous studies have revealed that several sporadic cancers express abundant MFG-E8, which contributes to the growth or invasion of tumors. However, nothing is known regarding MFG-E8 expression in sporadic colon cancer. In the present study, we investigated MFG-E8 expression in surgically resected human advanced colon cancer tissues. Representative images of immunohistochemistry findings are shown in Figure 6. MFG-E8 expression was clearly observed in colon cancers cells (Figure 6C-a and -b), whereas that was faintly seen in non-tumorous lesions (Fig 6C-c). Immunoreactive signals of MFG-E8 were also observed in mononuclear cells that had infiltrated around

the cancer cells (Fig. 6C-d). We also evaluated MFG-E8 expression in 17 advanced colon cancer specimens and found that the percentage of cases with positive findings was 73.0%. Notably, abundant expression was observed in the deeper invasive parts of the cancer tissues. In addition, we performed immunostaining for detection of MFG-E8 in adenoma (26 cases) and early cancer (23 cases) tumor tissues, and found that its expression rate in those was 18.2% and 57.0%, respectively. Thus, MFG-E8 expression in samples from human colon adenomas was shown to gradually increase from early to advanced cancer.

MFG-E8 stimulates epithelial cell proliferation via $\alpha_v\beta_3$ -integrin

Based on the results of our chimeric mice experiments, we next investigated whether MFG-E8 directly induces proliferation of colonic epithelial cells (Colon-26 cells) *in vitro*. Treatment with recombinant mouse MFG-E8 (rMFG-E8) significantly stimulated proliferation of Colon-26 cells (Fig. 7A), which was confirmed by the results of WST-1 assay (Fig. 7B). Finally, since the biological functions of MFG-E8 are dependent on the cell surface receptor $\alpha_v\beta_3$ -integrin, we also examined its role in MFG-E8-induced epithelial proliferation. Treatment with a neutralizing antibody (Fig. 7C) or siRNA (Fig. 7D) targeting α_v -integrin significantly reduced the proliferation of Colon-26 cells stimulated with rMFG-E8.

Discussion

In the present study, a deficiency of MFG-E8 reduced the incidence and size of colon tumors in a murine CAC model, though the severity of colonic inflammation became severe in MFG-E8 KO mice. On the other hand, experiments using a sporadic colon cancer model showed that MFG-E8 expression influenced tumor growth but not the incidence of tumor development. These findings indicate that MFG-E8 promotes tumor growth regardless of the presence or absence of colonic inflammation, whereas the development of colon tumors is initiated by MFG-E8 under inflammatory conditions.

In the present study, MFG-E8 deficiency exacerbated DSS-induced colitis, which supports our previous report showing the protective effects of rMFG-E8 in mice colitis models. The anti-inflammatory effects of MFG-E8 were also confirmed in I/R- and sepsis-induced intestinal injury models, and mainly dependent on the prompt clearance of apoptotic cells as well as an inhibition of inflammatory cytokines produced by macrophages (17-22). Apart from the anti-inflammatory effect, MFG-E8 directly regulates epithelial functions including proliferation and apoptosis. Chogle *et al.* reported that DSS administration induced more severe crypt-epithelial injury with delayed regeneration of colonic epithelium in MFG-E8 KO mice as compared to WT mice (17). In addition, Ajakaiye *et al.* found that rMFG-E8 treatment reduced radiation-induced intestinal mucosal damage with improved survival.

Enhancement of the proliferation and anti-apoptotic characteristics of epithelial cells contributes to decrease inflammation and induces repair of inflamed tissues. On the other hand, those functions also accelerate development of cancers under chronic inflammatory conditions (32, 34, 36-42). In the present study, we found that severe colitis developed in DSS-treated KO mice due to the lack of an anti-inflammatory effect

of MFG-E8. It is known that CAC development occurs more readily with severe colonic inflammation. However, the number of colon tumors that developed in the present KO mice was lower than that of those in the WT mice, indicating that MFG-E8 deficiency suppressed the potential of inflammation-induced cancer development even under severe colitis condition. PCNA has been identified as an antigen expressed in cell nuclei during the DNA synthesis phase of the cell cycle (G1 to S phase). To further confirm the influence of MFG-E8 on colonic epithelial proliferation, we determined the frequency of PCNA-positive epithelial cells in our DSS-induced colitis model and found that the number of those cells was significantly greater in WT mice as compared to KO mice, which was associated with colonic expression of MFG-E8. Ki67, a nuclear protein expressed from the G1 to M phase, is known as a cellular marker of proliferation. We also examined Ki67 expression in colonic tissues and found it to be increased in WT mice. A recent study showed that MFG-E8 regulates expression of cyclin-dependent kinase (CDK)-3 and enhances proliferation of mammary epithelial cells (25). On the other hand, p27 and p57 are CDK inhibitors that down-regulate the cell cycle and inhibit excess cell proliferation. We speculate that expression of those CDK inhibitors is accelerated in a homeostatic manner in response to increased epithelial cell proliferation, which may regulate initiation of the process of MFG-E8-related CAC development. We previously reported that MFG-E8 expression is upregulated in mononuclear cells infiltrating the lamina propria during the regeneration phase of DSS-induced colitis (14). A similar expression pattern was also found in human inflammatory colonic mucosa of UC patients (Fig. 6A). In addition, our present *in vitro* results clearly showed that MFG-E8 stimulates proliferation of colonic epithelial cells. Taken together, these findings suggest that MFG-E8 secreted by infiltrating inflammatory cells may stimulate

epithelial proliferation by regulating several cell cycle-related molecules in a paracrine manner during colitis, which might enhance the turnover of epithelial cells and initiate CAC development.

In the present study, it is possible that small latent cancer not found macroscopically or by stereoscopic microscopy did not grow to become overt cancer due to reduced cell proliferation in the CAC model KO mice. To examine this issue, sections with tumors (areas around the tumors) as well as serial sections were examined using a histological method. However, no small latent cancer areas or dysplastic epithelial lesions were found, suggesting that MFG-E8 contributes to initiation of CAC development. There are few reports regarding the correlation between MFG-E8 and cancer initiation markers. Ajakaiye *et al.* reported that treatment with rMFG-E8 increased the expression of p53, bcl-2, and p21 in intestinal epithelial cells, and also enhanced the anti-apoptotic function of those cells (23). Okuyama *et al.* revealed that p63, a member of the p53 family, stimulates MFG-E8 expression via p53-binding consensus sequences and/or related sites (43), which regulates various biological functions including cell proliferation. Although those findings suggest that the expression and function of MFG-E8 associated with p53 or p63 might initiate cancer development, further studies are necessary to clearly explain the role of MFG-E8 in initiation of CAC development.

A few studies that examined the role of MFG-E8 in cancer development without inflammatory stimuli have been presented. Sugano *et al.* investigated development of carcinogen-induced bladder cancer in MFG-E8 KO mice and found that the extent of tumors but not their incidence was significantly lower in KO mice as compared to WT mice (26). Neutzner *et al.* used Rip1-Tag2 transgenic mice, a model of

pancreas cancer, and established MFG-E8-deficient Rip1-Tag2 mice to examine the role of MFG-E8 in development and growth of pancreas cancer. Tumor growth in their model was lower as compared to the control (Rip1-Tag2 mice), though the incidence of tumors was similar between those strains (28). We also examined the influence of genetic MFG-E8 ablation on tumor incidence and growth in a sporadic colon cancer model without colitis induction in the present study. Similarly, though the average tumor size was lower in KO mice, we did not find any differences regarding tumor incidence between KO and WT mice. We also found that a deficiency of MFG-E8 significantly decreased tumor growth in the CAC model. Thus, MFG-E8 contributes to the promotion of tumor growth regardless of the presence or absence of inflammation.

Previous studies reported the overexpression of MFG-E8 in advanced tumor cells including breast, bladder, and pancreas cancers, which was associated with tumor growth, invasion, and metastasis (25-30). Tumor cells overexpressing MFG-E8 show a high growth potential as well as resistance to apoptosis induction in an autocrine manner, and silencing the MFG-E8 gene in those cells inhibits their growth (25, 27, 29). Although we examined MFG-E8 expression in colon tumors of experimental mice by immunohistochemistry, immunoreactive signals were not detected due to the low affinity of commercially available anti-mouse antibodies to the tissue samples. In this regard, we used surgically resected human colon cancer tissues for immunohistochemistry and found abundant expression of MFG-E8 in tumor and infiltrating mononuclear cells, suggesting that MFG-E8 may promote tumor growth mainly in autocrine as well as paracrine manners. On the other hand, other mechanisms regarding MFG-E8-mediated tumor growth have been reported. Increased expression of MFG-E8 in tumor cells also down-regulates E-cadherin expression, which promotes

metastasis by controlling epithelial-mesenchymal transition (EMT) (27). In addition to the direct effects of MFG-E8 on tumor cells, that secreted from tumor tissues induces angiogenesis by accelerating production of vascular endothelial growth factor (VEGF) (24, 28). Moreover, MFG-E8 induces the infiltration of Foxp3-positive regulatory T cells (Tregs) in tumor tissues, which increases the extent of tumor proliferation by down-regulating host tumor immunity (26, 27, 29, 30).

$\alpha_v\beta_3$ -integrin is expressed in a variety of cells including macrophages, epithelial cells, and endothelial cells (43). MFG-E8 binds to $\alpha_v\beta_3$ -integrin and contributes to various MFG-E8-induced biological events (6, 7). Bu *et al.* observed that treatment with rMFG-E8 enhanced migration of intestinal epithelial cells by activating intracellular protein kinase C (PKC), as well as reorganizing F-actin and Arp2/3 on the cells via $\alpha_v\beta_3$ -integrin (20). Silvestre *et al.* reported that MFG-E8 induces $\alpha_v\beta_3$ -integrin-dependent phosphorylation in endothelial cells and promotes VEGF-mediated neovascularization (24). In the present study, we clearly demonstrated that MFG-E8-induced proliferation of colonic epithelial cells was dependent on $\alpha_v\beta_3$ -integrin expression in those cells. However, further investigations are necessary to clarify the precise mechanisms regarding $\alpha_v\beta_3$ -integrin-dependent intracellular signaling in epithelial cells and its association with cancer development.

MFG-E8-blocking therapy may be a double-edged sword, as it may reduce carcinogenesis but enhance colonic inflammation. In this regard, MFG-E8 treatment should be performed to reduce colonic inflammation only in severe phases of UC, since long term maintenance with this therapy may accelerate CAC development. On the other hand, after development of CAC or sporadic cancers, blocking MFG-E8 function contributes to reduce tumor growth and metastasis by inhibiting cell proliferation and

angiogenesis. Further investigations regarding effectiveness and safety are necessary prior to clinical use of the therapy targeting MFG-E8.

In summary, we investigated the role of MFG-E8 in intestinal inflammation and its relationship to tumor development in a murine CAC model. The present results show that MFG-E8 expression is up-regulated in inflamed colonic tissues and initiates CAC development, which may be dependent on increased proliferation of epithelial cells via $\alpha_v\beta_3$ -integrin. Furthermore, MFG-E8 promoted tumor growth in both our CAC and sporadic colon cancer models. These results are the first to show the role of MFG-E8 in the pathogenesis of colon cancer. For development of a novel therapy targeting MFG-E8, additional findings regarding the various physiological, immunological, and clinical aspects must be evaluated in the future.

References

1. Krysko DV, D'Herde K, Vandenabeele P. Clearance of apoptotic and necrotic cells and its immunological consequences. *Apoptosis*. 2006;11:1709-26.
2. Nagata S, Hanayama R, Kawane K. Autoimmunity and the clearance of dead cells. *Cell*. 2010;140:619-30.
3. Gregory CD, Devitt A. The macrophage and the apoptotic cell: an innate immune interaction viewed simplistically. *Immunol*. 2004;113:1-14.
4. Lauber K, Blumenthal SG, Waibel M, Wesselborg S. Clearance of apoptotic cells: getting rid of the corpses. *Mol Cell*. 2004;14:277-87.
5. Savill J, Fadok V. Corpse clearance defines the meaning of cell death. *Nature*. 2000;407:784-8.
6. Miyasaka K, Hanayama R, Tanaka M, Nagata S. Expression of milk fat globule epidermal growth factor 8 in immature dendritic cells for engulfment of apoptotic cells. *Eur J Immunol*. 2004;34:1414-22.
7. Hanayama R, Tanaka M, Miwa K, Shinohara A, Iwamatsu A, Nagata S. Identification of a factor that links apoptotic cells to phagocytes. *Nature*. 2002;417:182-7.
8. Asano K, Miwa M, Miwa K, Hanayama R, Nagase H, Nagata S, et al. Masking of phosphatidylserine inhibits apoptotic cell engulfment and induces autoantibody production in mice. *J Exp Med*. 2004;200:459-67.
9. Hanayama R, Tanaka M, Miyasaka K, Aozasa K, Koike M, Uchiyama Y, et al. Autoimmune disease and impaired uptake of apoptotic cells in MFG-E8-deficient mice. *Science*. 2004;304:1147-50.

10. Ait-Oufella H, Kinugawa K, Zoll J, Simon T, Boddaert J, Heeneman S, et al. Lactadherin deficiency leads to apoptotic cell accumulation and accelerated atherosclerosis in mice. *Circulation*. 2007;115:2168-77.
11. Thorp E, Tabas I. Mechanisms and consequences of efferocytosis in advanced atherosclerosis. *J Leukoc Biol*. 2009;86:1089-95.
12. Fuller AD, Van Eldik LJ. MFG-E8 regulates microglial phagocytosis of apoptotic neurons. *J Neuroimmune Pharmacol*. 2008;3:246-56.
13. Kusunoki R, Ishihara S, Aziz M, Oka A, Tada Y, Kinoshita Y. Roles of milk fat globule-epidermal growth factor 8 in intestinal inflammation. *Digestion*. 2012;85:103-7.
14. Aziz MM, Ishihara S, Mishima Y, Oshima N, Moriyama I, Yuki T, et al. MFG-E8 attenuates intestinal inflammation in murine experimental colitis by modulating osteopontin-dependent α v β 3 integrin signaling. *J Immunol*. 2009;182:7222-32.
15. Otani A, Ishihara S, Aziz MM, Oshima N, Mishima Y, Moriyama I, et al. Intrarectal administration of milk fat globule epidermal growth factor-8 protein ameliorates murine experimental colitis. *Int J Mol Med*. 2012;29:349-56.
16. Mishiro T, Kusunoki R, Otani A, Ansary MM, Tongu M, Harashima N, et al. Butyric acid attenuates intestinal inflammation in murine DSS-induced colitis model via milk fat globule-EGF factor 8. *Lab Invest*. 2013;93:834-43.
17. Chogle A, Bu HF, Wang X, Brown JB, Chou PM, Tan XD. Milk fat globule-EGF factor 8 is a critical protein for healing of dextran sodium sulfate-induced acute colitis in mice. *Mol Med*. 2011;17:502-7.

18. Komura H, Miksa M, Wu R, Goyert SM, Wang P. Milk fat globule epidermal growth factor-factor VIII is down-regulated in sepsis via the lipopolysaccharide-CD14 pathway. *J Immunol.* 2009;182:581-7.
19. Cui T, Miksa M, Wu R, Komura H, Zhou M, Dong W, et al. Milk fat globule epidermal growth factor 8 attenuates acute lung injury in mice after intestinal ischemia and reperfusion. *Am J Respir Crit Care Med.* 2010;181:238-46.
20. Bu HF, Zuo XL, Wang X, Ensslin MA, Koti V, Hsueh W, et al. Milk fat globule-EGF factor 8/lactadherin plays a crucial role in maintenance and repair of murine intestinal epithelium. *J Clin Invest.* 2007;117:3673-83.
21. Wu R, Dong W, Wang Z, Jacob A, Cui T, Wang P. Enhancing apoptotic cell clearance mitigates bacterial translocation and promotes tissue repair after gut ischemia-reperfusion injury. *Int J Mol Med.* 2012;30:593-8.
22. Zhao QJ, Yu YB, Zuo XL, Dong YY, Li YQ. Milk fat globule-epidermal growth factor 8 is decreased in intestinal epithelium of ulcerative colitis patients and thereby causes increased apoptosis and impaired wound healing. *Mol Med.* 2012;18:497-506.
23. Ajakaiye MA, Jacob A, Wu R, Yang WL, Nicastro J, Coppa GF, et al. Recombinant human MFG-E8 attenuates intestinal injury and mortality in severe whole body irradiation in rats. *PLoS One.* 2012;7:e46540.
24. Silvestre JS, Théry C, Hamard G, Boddaert J, Aguilar B, Delcayre A, et al. Lactadherin promotes VEGF-dependent neovascularization. *Nat Med.* 2005;11:499-506.
25. Carrascosa C, Obula RG, Missiaglia E, Lehr HA, Delorenzi M, Frattini M, et al. MFG-E8/lactadherin regulates cyclins D1/D3 expression and enhances the

- tumorigenic potential of mammary epithelial cells. *Oncogene*. 2012;31:1521-32.
26. Sugano G, Bernard-Pierrot I, Laé M, Battail C, Allory Y, Stransky N, et al. Milk fat globule--epidermal growth factor--factor VIII (MFG-E8)/lactadherin promotes bladder tumor development. *Oncogene*. 2011;30:642-53.
27. Jinushi M, Nakazaki Y, Carrasco DR, Draganov D, Souders N, Johnson M, et al. Milk fat Globule EGF-8 promotes melanoma progression through coordinated Akt and Twist signaling in the tumor microenvironment. *Cancer res*. 2008;68: 8889-98.
28. Neutzner M, Lopez T, Feng X, Bergmann-Leitner ES, Leitner WW, Udey MC. MFG-E8/lactadherin promotes tumor growth in an angiogenesis-dependent transgenic mouse model of multistage carcinogenesis. *Cancer Res*. 2007;67:6777-85.
29. Jinushi M, Sato M, Kanamoto A, Itoh A, Nagai S, Koyasu S, et al. Milk fat globule epidermal growth factor-8 blockade triggers tumor destruction through coordinated cell-autonomous and immune-mediated mechanisms. *J Exp Med*. 2009;206:1317-26.
30. Jinushi M, Nakazaki Y, Dougan M, Carrasco DR, Mihm M, Dranoff G. MFG-E8-mediated uptake of apoptotic cells by APCs links the pro- and antiinflammatory activities of GM-CSF. *J Clin Invest*. 2007;117:1902-13.
31. Moriyama I, Ishihara S, Rumi MA, Aziz MD, Mishima Y, Oshima N, et al. Decoy oligodeoxynucleotide targeting activator protein-1 (AP-1) attenuates intestinal inflammation in murine experimental colitis. *Lab Invest*. 2008;88:652-63.
32. Suzuki R, Kohno H, Sugie S, Nakagama H, Tanaka T. Strain differences in the susceptibility to azoxymethane and dextran sodium sulfate-induced colon carcinogenesis in mice. *Carcinogenesis*. 2006;27:162-9.

33. Tanaka T, Kohno H, Sakata K, Yamada Y, Hirose Y, Sugie S, et al. Modifying effects of dietary capsaicin and rotenone on 4-nitroquinoline 1-oxide-induced rat tongue carcinogenesis. *Carcinogenesis*. 2002;8:1361-7.
34. Neufert C, Becker C, Neurath MF. An inducible mouse model of colon carcinogenesis for the analysis of sporadic and inflammation-driven tumor progression. *Nat Protoc*. 2007;2:1998-2004.
35. Endo H, Hosono K, Uchiyama T, Sakai E, Sugiyama M, Takahashi H, et al. Leptin acts as a growth factor for colorectal tumours at stages subsequent to tumour initiation in murine colon carcinogenesis. *Gut*. 2011;60:1363-71.
36. Rosenberg DW, Giardina C, Tanaka T. Mouse models for the study of colon carcinogenesis. *Carcinogenesis*. 2009;30:183-96.
37. Eaden JA, Abrams KR, Mayberry JF. The risk of colorectal cancer in ulcerative colitis: a meta-analysis. *Gut*. 2001;48:526-35.
38. Ullman TA, Itzkowitz SH. Intestinal inflammation and cancer. *Gastroenterology*. 2011;140:1807-16.
39. Cooper HS, Everley L, Chang WC, Pfeiffer G, Lee B, Murthy S, et al. The role of mutant Apc in the development of dysplasia and cancer in the mouse model of dextran sulfate sodium-induced colitis. *Gastroenterology*. 2001;121:1407-16.
40. Greten FR, Eckmann L, Greten TF, Park JM, Li ZW, Egan LJ, et al. IKKbeta links inflammation and tumorigenesis in a mouse model of colitis-associated cancer. *Cell*. 2004;118:285-96.
41. Grivennikov S, Karin E, Terzic J, Mucida D, Yu GY, Vallabhapurapu S, et al. IL-6 and Stat3 are required for survival of intestinal epithelial cells and development of colitis-associated cancer. *Cancer Cell*. 2009;15:103-13.

42. Grivennikov SI, Greten FR, Karin M. Immunity, inflammation, and cancer. *Cell*. 2010;140:883-99.
43. Okuyama T, Kurata S, Tomimori Y, Fukunishi N, Sato S, Osada M, *et al.* p63(TP63) elicits strong trans-activation of the MFG-E8/lactadherin/BA46 gene through interactions between the TA and DeltaN isoforms. *Oncogene*. 2008;27:308-317.
44. Avraamides CJ, Garmy-Susini B, Varner JA. Integrins in angiogenesis and lymphangiogenesis. *Nat Rev Cancer*. 2008;8:604-17.

Figure legends

Figure 1

The natural course of MFG-E8 KO mice under physiological conditions was similar to that of WT mice. (A) Age-related BW changes (5-30 weeks old) in KO (n=4) and WT (n=4) mice. Representative images show colon length (B, 6 weeks; C, 30 weeks) and histology (D, 6 weeks; E, 30 weeks), and immunohistochemistry for PCNA (30 weeks). (G) Average numbers of PCNA-positive epithelial cells (KO, n=6; WT, n=6).

Figure 2

DSS-induced colitis was found to be exacerbated in MFG-E8 KO mice. Experimental colitis models were established by administering a 2.5% DSS solution in drinking water for 10 days (WT, n=7; KO, n=7). (A) BW changes in WT and KO mice with DSS-induced colitis (B) Representative image showing colon lengths. (C) Average colon lengths. (D) Representative images showing inflamed colon histology. (E) Average histological scores. (F, G) Cytokine mRNA and protein levels in colonic tissues. * $p < 0.05$ vs. WT. ** $p < 0.01$ vs. WT.

Figure 3

In the CAC model, MFG-E8 KO mice developed fewer tumors and showed reduced tumor size as compared to the WT mice. (A) Schematic overview of CAC model. Mice were injected with AOM (10 mg/kg) in an intraperitoneal manner, followed by a single cycle of DSS (2.0%, 7 days) in drinking water and euthanized at 18 weeks. (B) Tumor morphology shown by stereoscopic microscopy (upper, 0.2% methylene blue staining) and histology (lower, hematoxyline-eosin staining). (C) Average number and size of

tumors per mouse in WT (n=12) and MFG-E8 KO (n=10) mice. *****p* <0.01 vs. WT, **p* <0.05 vs. WT.**

Figure 4

MFG-E8 was up-regulated during colonic inflammation, while the proliferation of colon epithelial cells was lower in MFG-E8 KO mice as compared to the WT mice. (A) Schematic overview of chronic DSS colitis model. Mice were given 2.5% DSS in drinking water for 7 days, followed by 14 days of regular water. (B) Time-course change of MFG-E8 mRNA expression in colon tissues (n=4/group). ****p* <0.05 vs. control.** (C) Representative images showing PCNA staining in the histological sections during the recovery phase of DSS colitis (3 weeks). (D) Average PCNA-positive cells per colon crypt (3 weeks, blank bar: WT, black bar: KO). N=4; KO, N=4. ****p* <0.05 vs. WT.**

Figure 5

In the sporadic cancer model, tumors developed in MFG-E8 KO mice were smaller than those in WT mice. (A) Schematic overview of sporadic cancer model. Mice were injected with AOM (10 mg/kg) in an intraperitoneal manner weekly for 6 weeks and euthanized at 31 weeks. (B) Tumor morphology shown by stereoscopic microscopy (upper, 0.2% methylene blue staining) and histology (lower, hematoxyline-eosin staining). (C) Average number and size of tumors in WT (n=26) and MFG-E8 KO (n=21) mice. ****p* <0.05 vs. WT.**

Figure 6

(A) Increased expression of MFG-E8 in mononuclear cells infiltrating the active

mucosa of UC patients. Representative immunohistochemical images of MFG-E8 expression. (B) MFG-E8 mRNA levels in active and inactive colonic tissues. $p < 0.01$ vs. inactive. (C) Abundant expression of MFG-E8 in human colon cancer. Surgically resected human colon cancer tissues were obtained and MFG-E8 expression was examined by immunohistochemistry. Representative images of MFG-E8 expression in colon cancer cells (a, b), a non-tumorous lesion (c), and infiltrating mononuclear cells (d).

Figure 7

MFG-E8 was found to promote epithelial cell proliferation via $\alpha_v\beta_3$ -integrin. (A, B) Colon-26 cells (2×10^5 /well) were seeded and treated with rMFG-E8 (400 ng/ml) for 24 hours. Cells were counted and a WST-1 assay was assessed. $*p < 0.05$ vs. PBS. Error bars indicate SEM values obtained from 3 independent experiments. (C, D) Colon-26 cells (2×10^5 /well) were seeded and pre-treated with the neutralizing antibody for α_v -integrin (400 ng/ml) for 3 hours or siRNA targeting α_v -integrin for 24 hours, then treated with rMFG-E8 (100 or 800 ng/ml) for 24 hours. The effect of rMFG-E8 (100 ng/ml) was assessed by a WST-1 assay. $*p < 0.05$, $**p < 0.01$ vs. PBS or control antibody. Error bars indicate SEM values obtained from 3 independent experiments.

Supplemental Table 1.

Primer sequences used for real-time PCR.

Supplemental Figure 1.

Colon epithelial cell proliferation was lower in MFG-E8 KO mice as compared to WT mice. (A) Representative images showing ki67 staining in histological sections during recovery phase of DSS colitis (3 weeks). (B) Average number of ki67-positive cells per colon crypt (3 weeks, blank bar: WT, black bar: KO). (WT, n=4; KO, n=4. * $p < 0.05$ vs. WT.

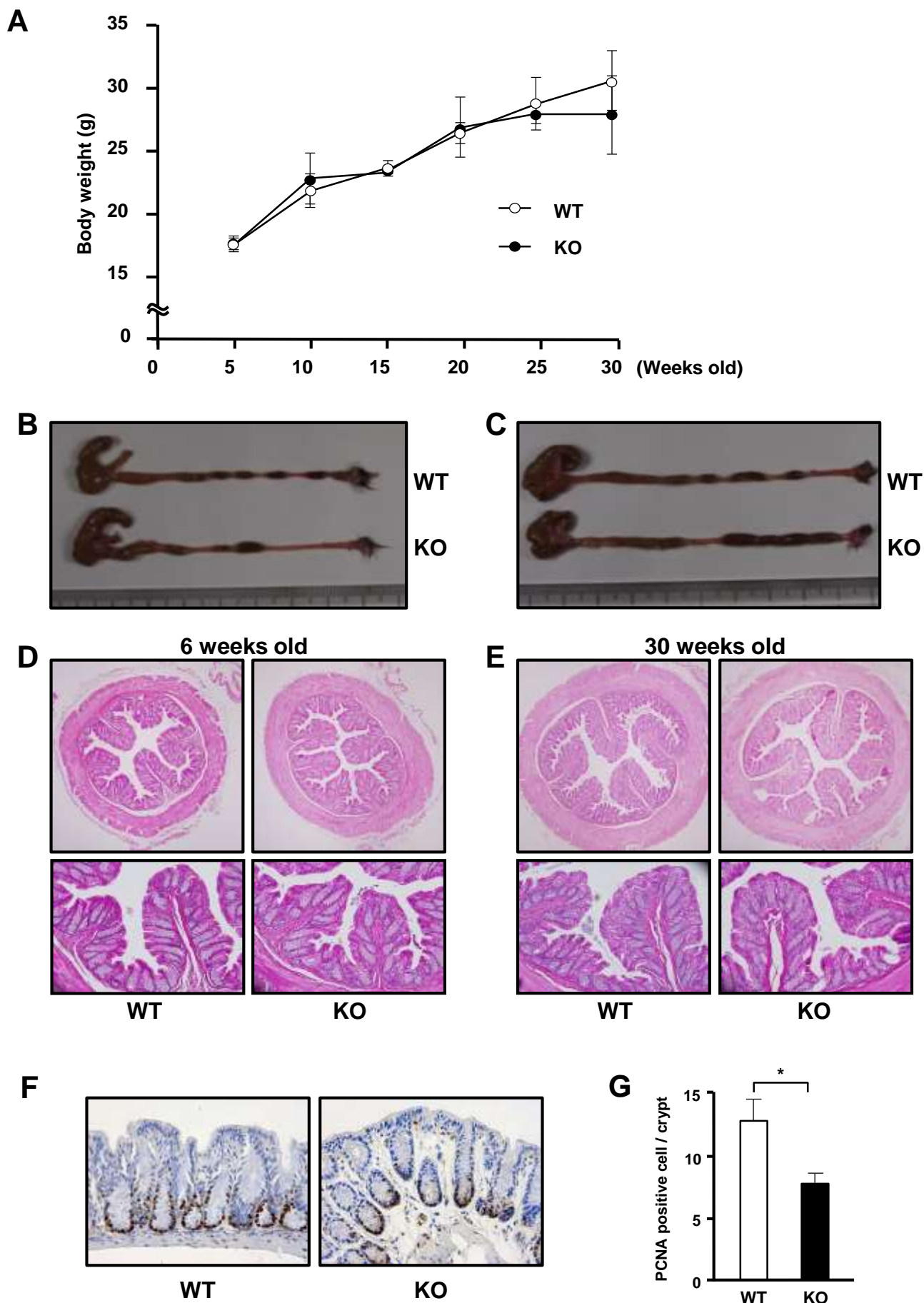
Table 1. Primer sequences.

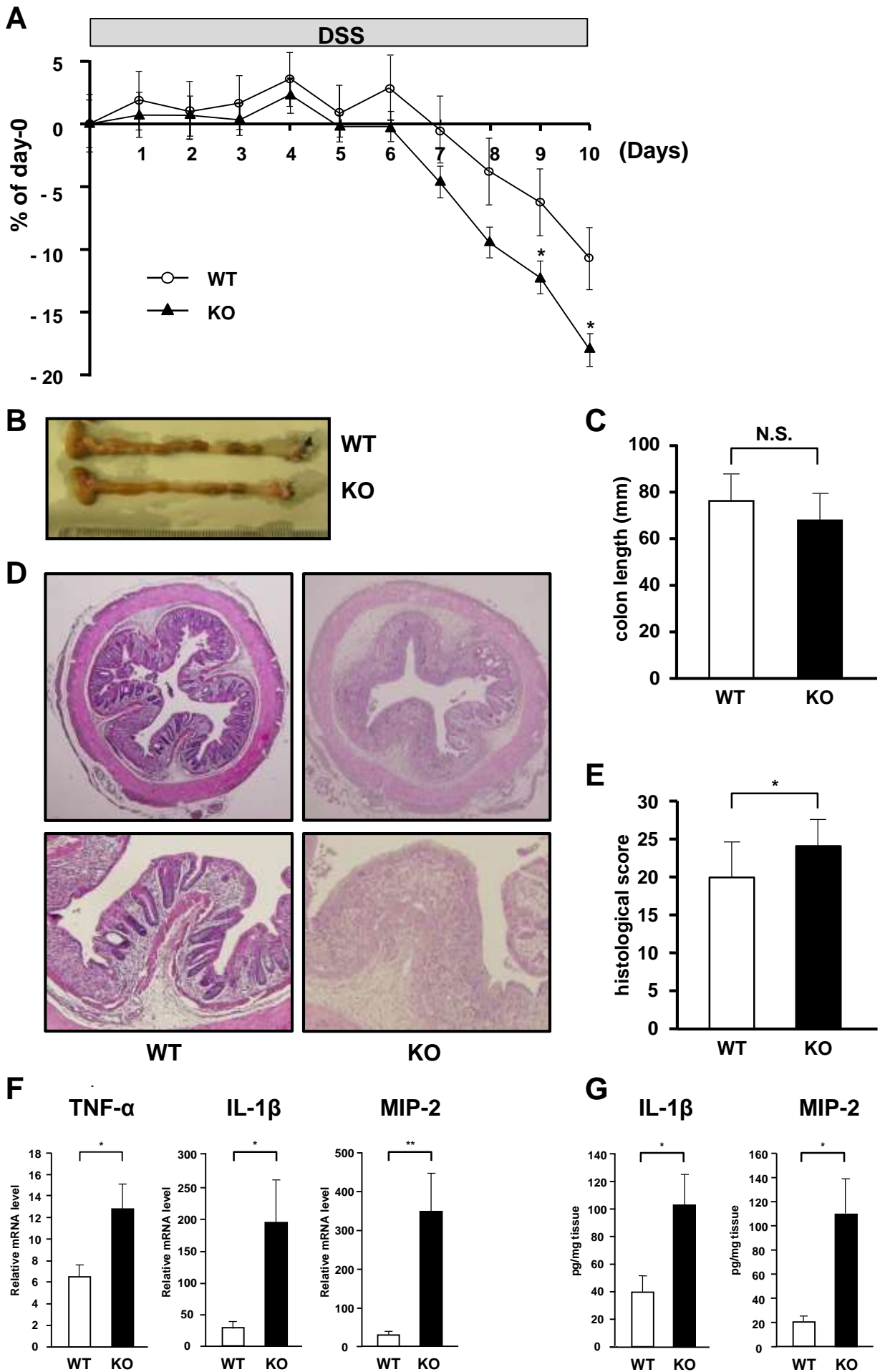
Gene		Sequences (5`-3`)
MFG-E8	Forward:	CGGGCCAAGACAATGACATC
	Reverse:	TCTCTCAGTCTCATTGCACACAAG
MFG-E8 (human)	Forward:	GGAGATGTCTTCCCCTCGTACAC
	Reverse:	AGATGAGGCGGCGATCTG
TNF- α	Forward:	AGACCCTCACACTCAGATCATCTTC
	Reverse:	TCCTCCACTTGGTGGTTTG
IL-1 β	Forward:	AGGCTCCGAGATGAACAACA
	Reverse:	TTGGGATCCCACTCTCCA
MIP-2	Forward:	TCCAGAGCTTGAGTGTGACG
	Reverse:	GCCCTTGAGAGTGGCTATGA
GAPDH	Forward:	ACCCAGAAGACTGTGGATGG
	Reverse:	GGTCCTCAGTGTAGCCCAAG

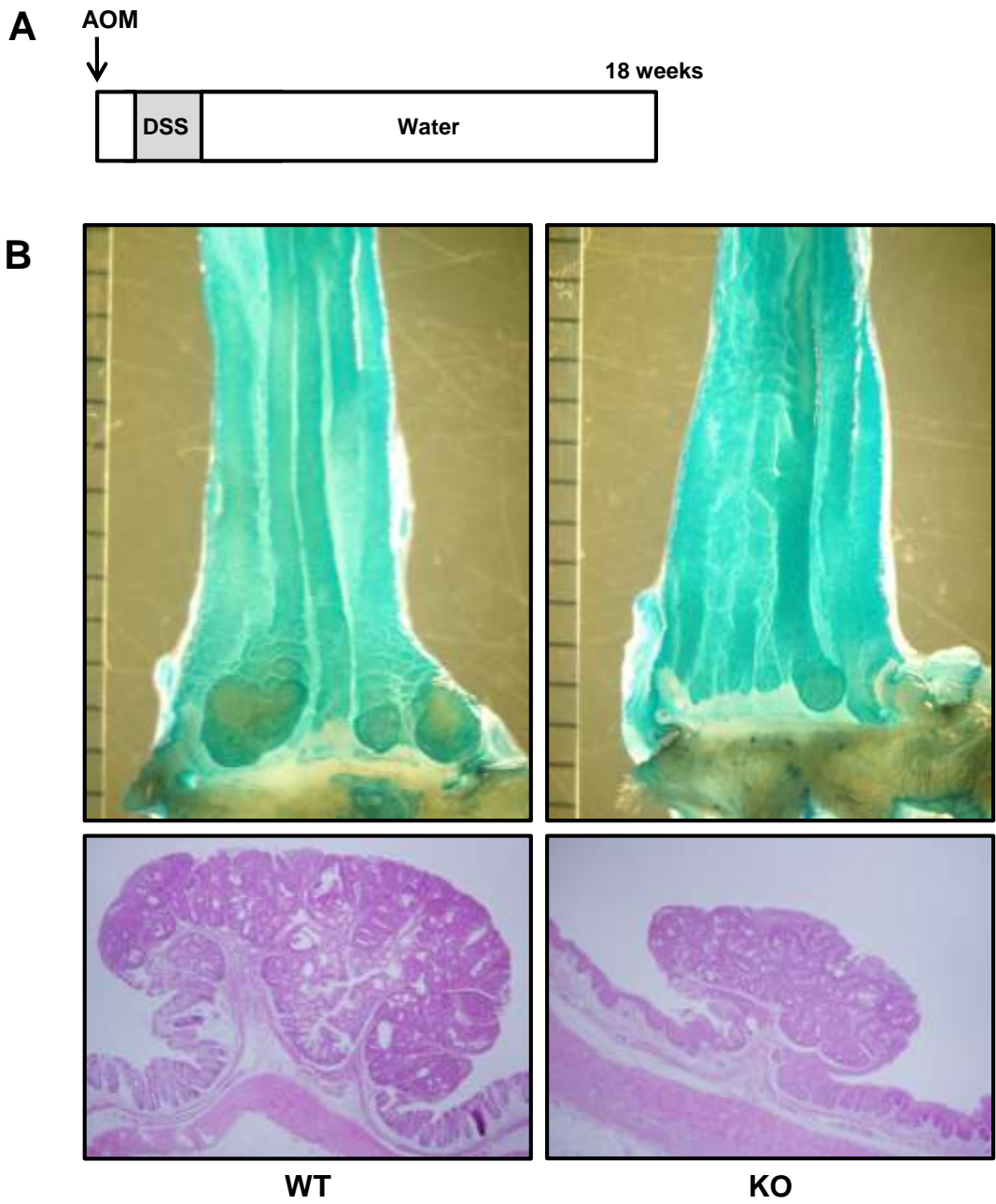
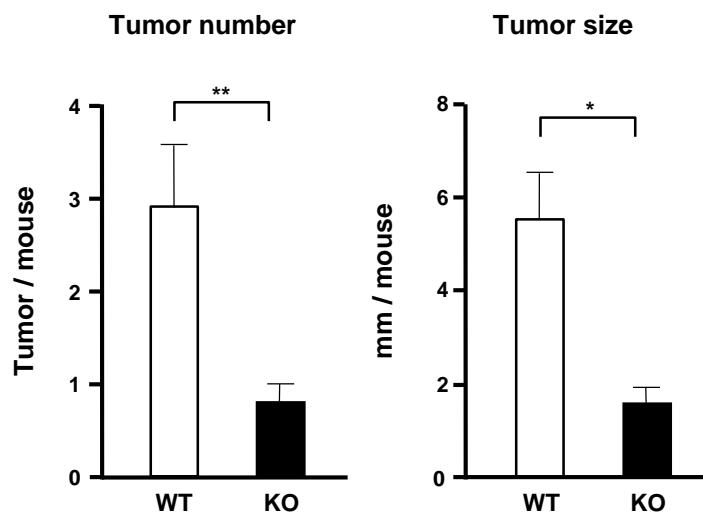
TNF, tumor necrosing factor; IL, interleukin;

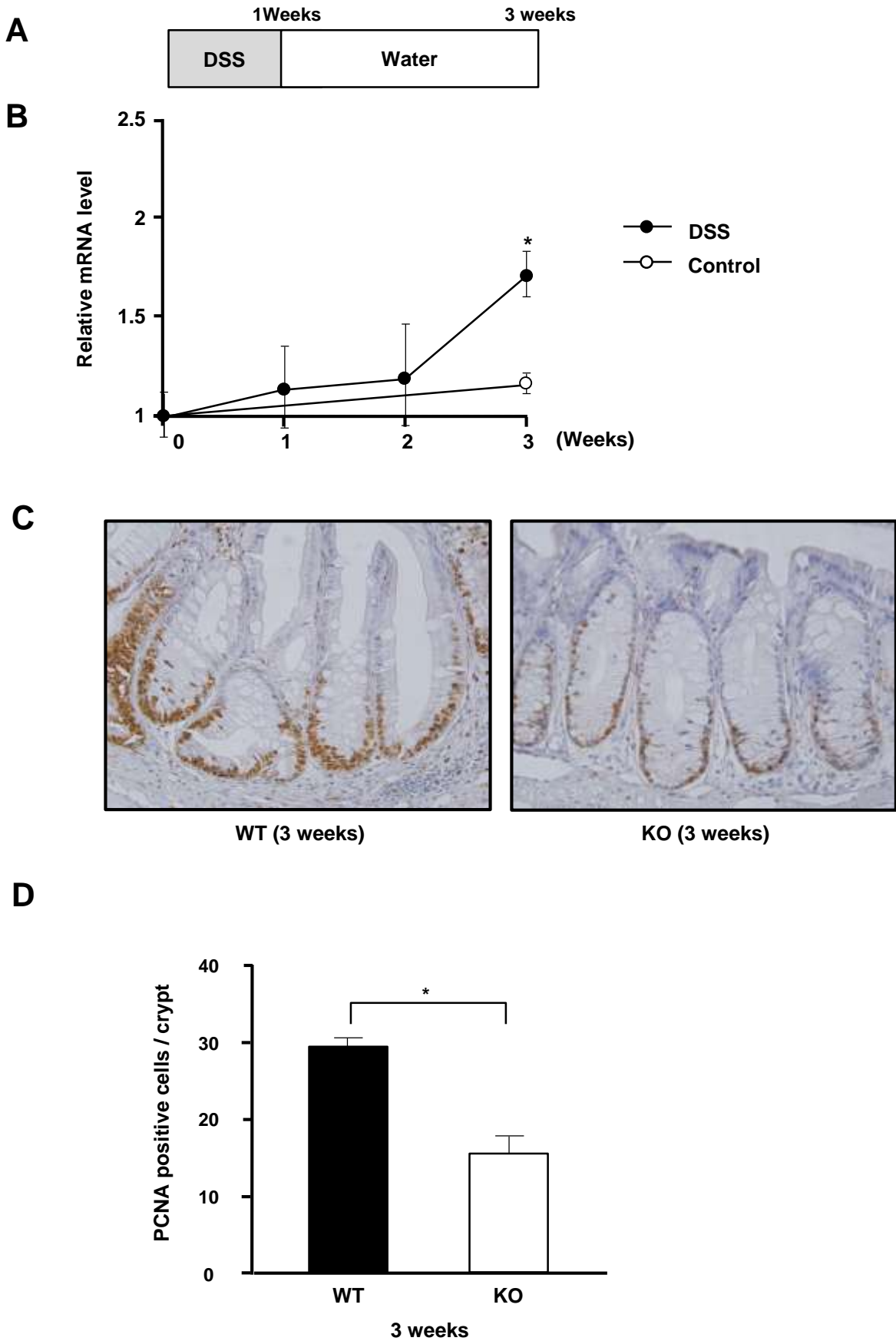
MIP, macrophage inflammatory protein;

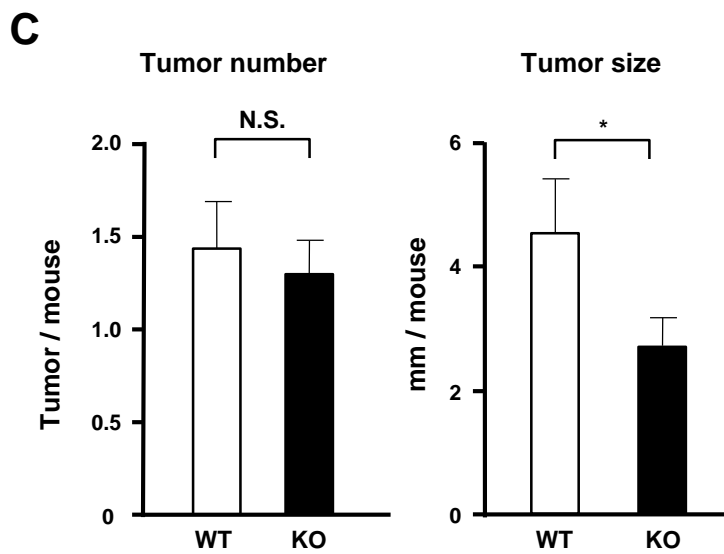
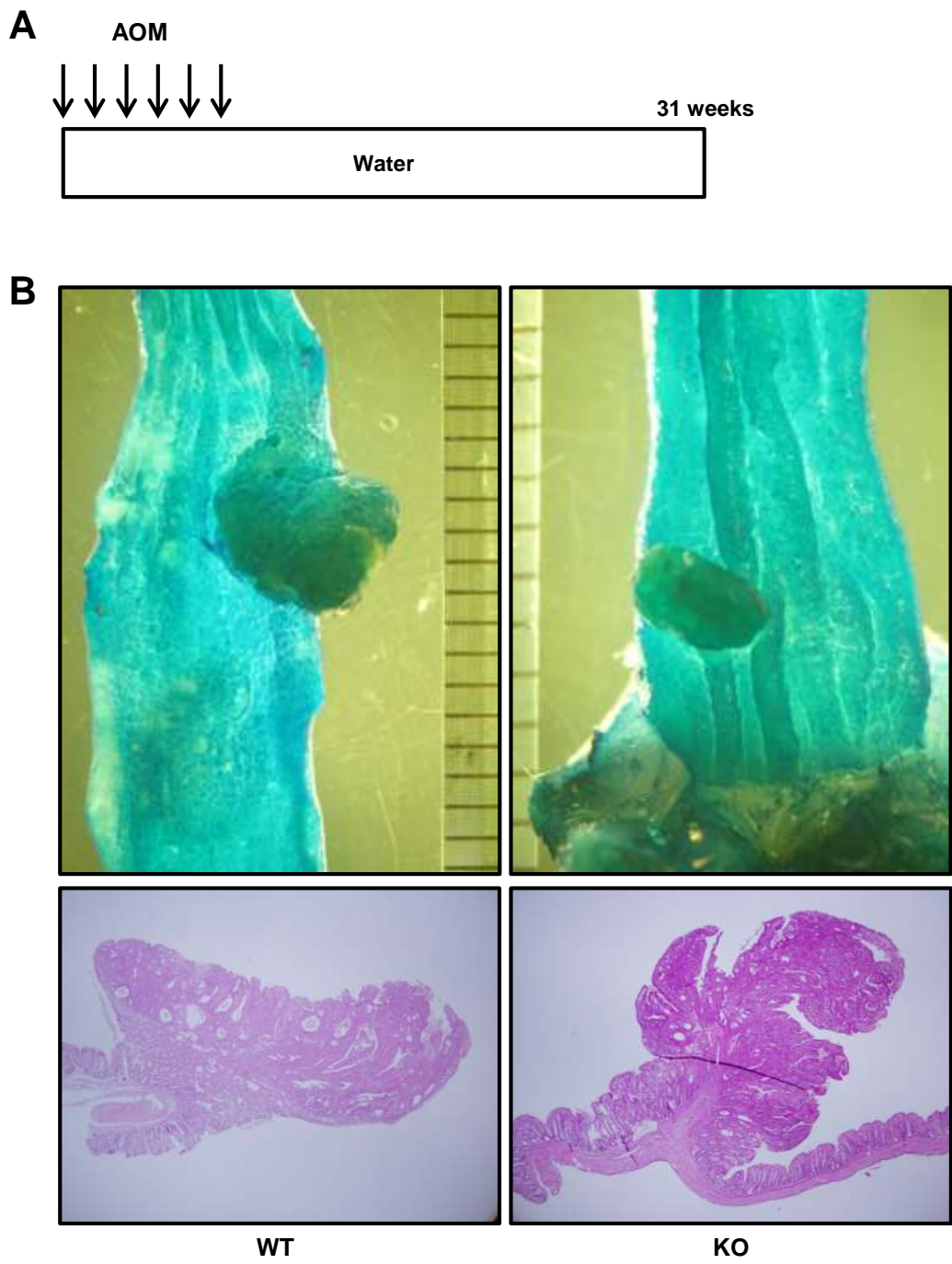
GAPDH, glyceraldehyde-3-phosphate dehydro genase.



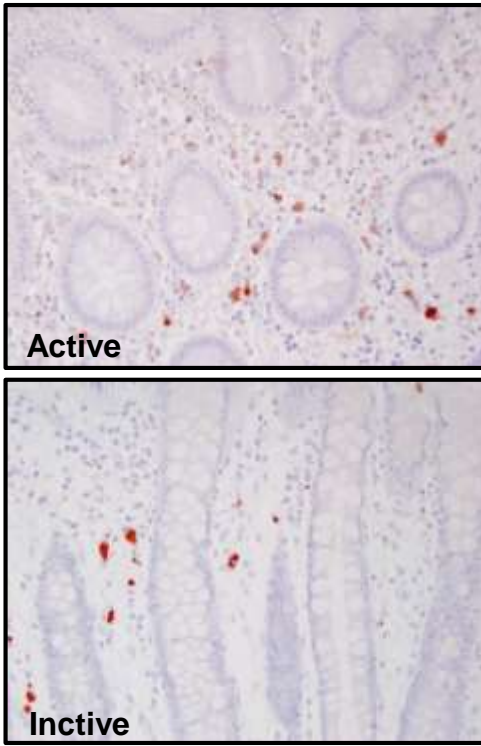


**C**

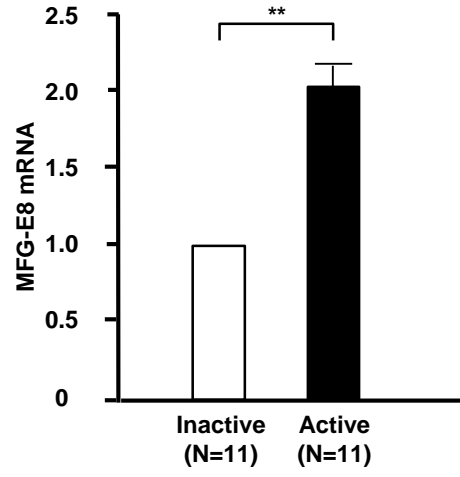




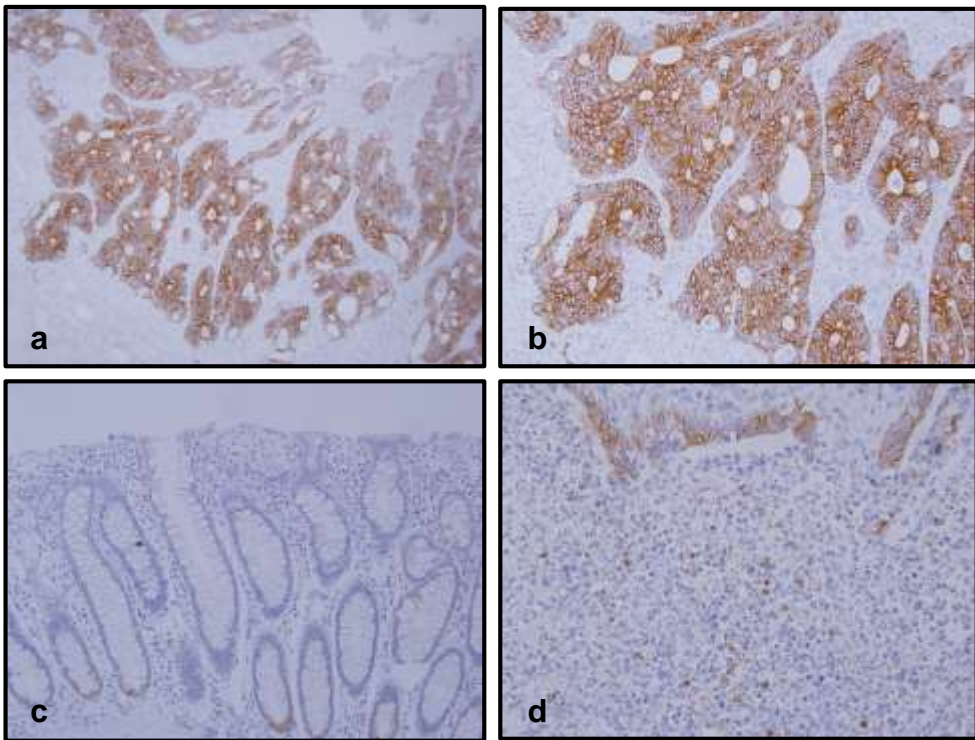
A

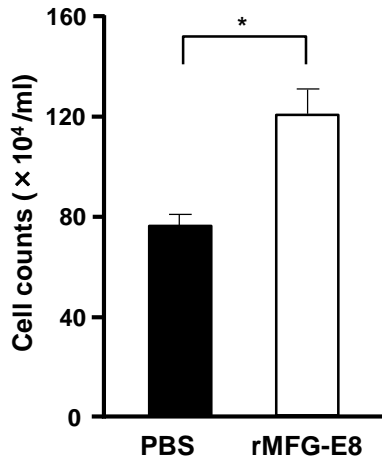
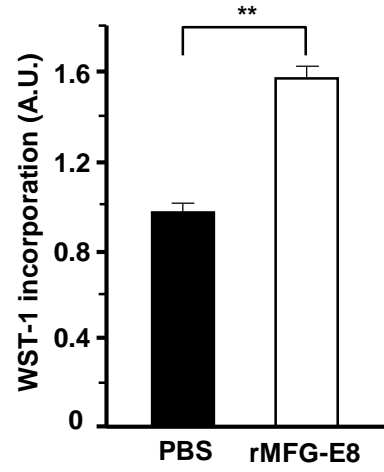
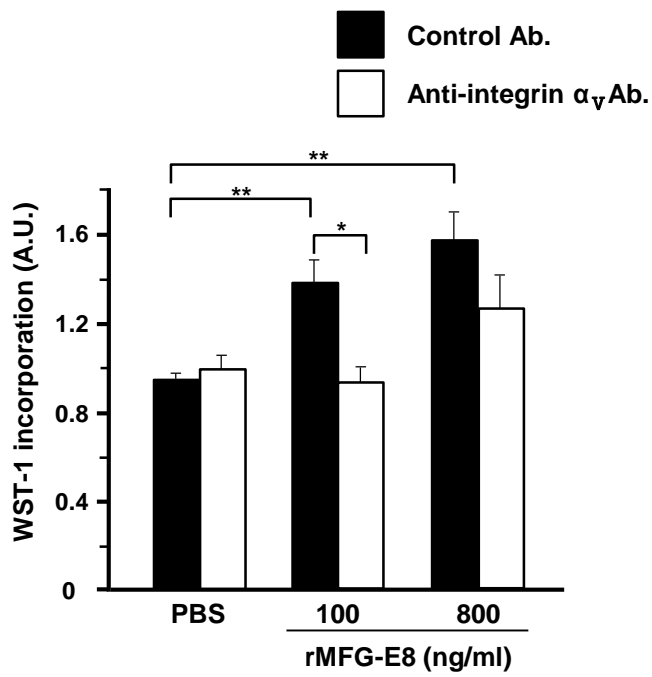
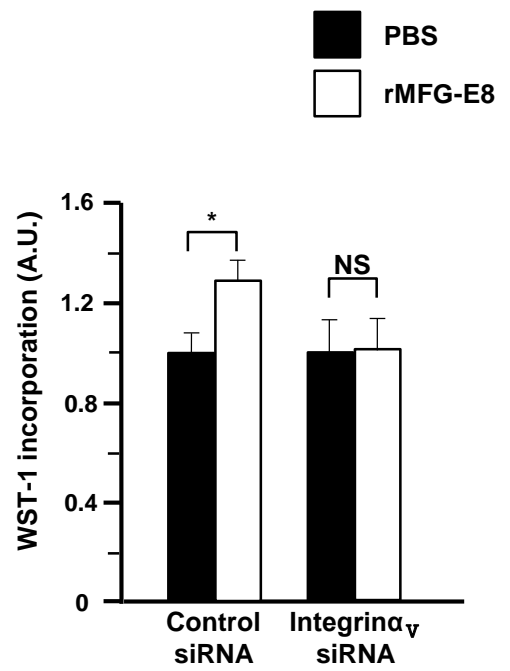


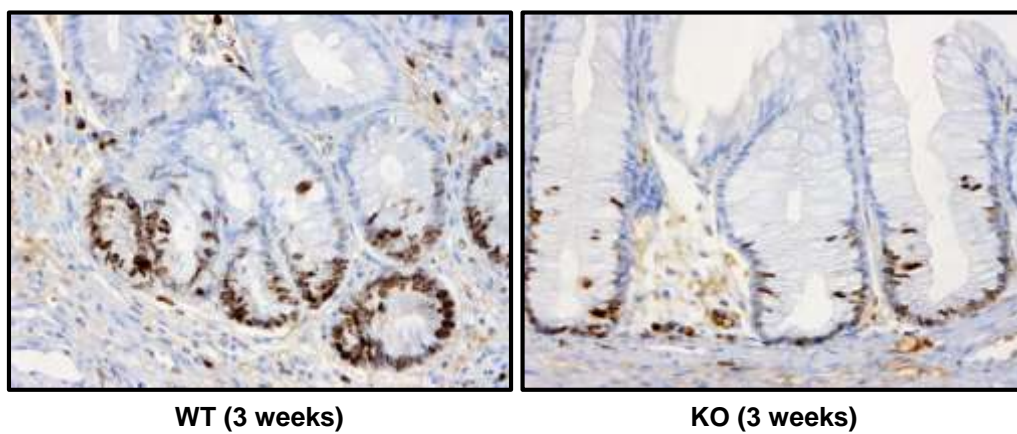
B



C



A**B****C****D**

A**B**